

NBSIR 73-322
(AFAPL-TR-73-37)

FORCED CONVECTION HEAT TRANSFER TO SUBCRITICAL HELIUM I

Patricia J. Giarrantano
R. C. Hess
M. C. Jones

Cryogenics Division
Institute for Basic Standards
National Bureau of Standards
Boulder, Colorado 80302

May 1973

Interim Report

Prepared for
AIR FORCE AERO PROPULSION LABORATORY
Air Force Systems Command
Wright-Patterson Air Force Base, Ohio 45433

NBSIR 73-322
(AFAPL-TR-73-37)

FORCED CONVECTION HEAT TRANSFER TO SUBCRITICAL HELIUM I

Patricia J. Giarrantano
R. C. Hess
M. C. Jones

Cryogenics Division
Institute for Basic Standards
National Bureau of Standards
Boulder, Colorado 80302

May 1973

Interim Report

Prepared for
AIR FORCE AERO PROPULSION LABORATORY
Air Force Systems Command
Wright-Patterson Air Force Base, Ohio 45433



U.S. DEPARTMENT OF COMMERCE, Frederick B. Dent, Secretary
NATIONAL BUREAU OF STANDARDS, Richard W. Roberts, Director

NOTICE

When Government drawings, specifications, or other data are used for any purpose other than in connection with a definitely related Government procurement operation, the United States Government thereby incurs no responsibility nor any obligation whatsoever; and the fact that the government may have formulated, furnished, or in any way supplied the said drawings, specifications, or other data, is not to be regarded by implication or otherwise as in any manner licensing the holder or any other person or corporation, or conveying any rights or permission to manufacture, use, or sell any patented invention that may in any way be related thereto.

Copies of this report should not be returned unless return is required by security considerations, contractual obligations, or notice on a specific document.

FOREWORD

The work described in this report was begun under the sponsorship of the U.S. Atomic Energy Commission (Contract Agreement AT(49-2)-1165) as part of the Helium Heat Transfer program of the National Bureau of Standards begun in 1968. Previous reports have covered NBS work on heat transfer to supercritical helium I, Kapitza conductance, viscosity of helium I and other thermophysical properties of helium I. This phase of the program was completed under sponsorship of the Department of the Air Force, Wright-Patterson Air Force Base, and was funded with FY-1972 AF Aero Propulsion Laboratory Director's Funds.

This Technical Report has been reviewed and is approved for publication.



Dr. C. E. Oberly/GS-12

APPROVED:



Dr. P. E. Stover/GS-14

CONTENTS

1.	INTRODUCTION	1
2.	DESCRIPTION OF EXPERIMENTAL APPARATUS AND MEASUREMENT	1
2.1	Test Section	2
2.2	Temperature Measurement	2
2.3	Pressure and Flow Measurement	7
2.4	Extraneous Heat Exchange	8
2.5	Experimental Measurement	8
3.	HEAT TRANSFER RESULTS	10
3.1	Wall Temperature Profiles	10
3.2	Critical Heat Flux	23
3.3	Comparison of Modes of Heat Transfer	30
4.	PERFORMANCE OF CENTRIFUGAL PUMP WHILE CIRCULATING LIQUID HELIUM	32
5.	CONCLUSIONS	35
6.	REFERENCES	36

FIGURES

Figure 1.	Schematic of the boiling heat transfer flow loop.	3
Figure 2.	Sketch of mounting scheme for carbon resistance thermometers	4
Figure 3.	Wall temperature profile for test section	11
Figure 4.	Wall temperature profile for test section	12
Figure 5.	Wall temperature profile for test section	13
Figure 6.	Wall temperature profile for test section	14
Figure 7.	Wall temperature profile for test section	15
Figure 8.	Wall temperature profile for test section	16

FIGURES (CONTINUED)

Figure 9.	Wall temperature profile for test section	17
Figure 10.	Wall temperature profile for test section	18
Figure 11.	Heat flux vs temperature difference for station 1	19
Figure 12.	Heat flux vs temperature difference for station 10	20
Figure 13.	Comparison of subcritical and supercritical wall temperature profiles under similar mass velocity and heat flux conditions	22
Figure 14.	Critical heat flux as a function of length to diameter ratio with pressure and mass velocity as parameters	25
Figure 15.	Heat transfer coefficient as a function of quality with mass velocity and pressure as parameters	27
Figure 16.	Heat transfer coefficient as a function of quality (comparison of this study's data with that of reference 4)	29
Figure 17.	Comparison of modes of helium heat transfer	31
Figure 18.	Pump performance characteristics and flow loop load line	33
Figure 19.	Ratio of measured flow rate to flow rate predicted from centrifugal pump performance characteristics vs subcooling power	34

ABSTRACT

Preliminary results of an experimental investigation of heat transfer to liquid helium under forced flow conditions are reported for a 0.213 cm i. d. x 10 cm long test section subject to the following range of operating conditions:

System pressures	1.1 - 2.1 atm
Mass velocities	4 - 64 g/s-cm ²
Heat fluxes	0.04 - 0.53 W/cm ²
Inlet subcooling	0.03 - 0.10 K

The effect of the above system parameters on the heat transfer and critical heat flux is discussed; a comparison of forced convection boiling with other modes of heat transfer (pool boiling and supercritical) and the performance of a centrifugal pump used for circulating the liquid helium are also included in the report.

Key Words: centrifugal pump; critical heat flux; film boiling; forced convection; heat transfer; helium; nucleate boiling; subcritical; supercritical.

FORCED CONVECTION HEAT TRANSFER TO SUBCRITICAL HELIUM I

1. INTRODUCTION

In a previous study by Giarratano, Arp and Smith [1] at the Cryogenics Division of NBS, Boulder, Colorado, heat transfer coefficients for forced flow of supercritical helium were measured and a correlation was developed to predict the heat transfer in this region. As an extension of that study this report describes the preliminary experimental results obtained for forced convection heat transfer in the subcritical region, i. e. , below the critical pressure 2. 245 atm.* Operation of the centrifugal pump, used for circulation of helium around the test loop in the subcritical region, will also be discussed.

2. DESCRIPTION OF EXPERIMENTAL APPARATUS AND MEASUREMENT

A schematic of the boiling heat transfer flow loop is shown in figure 1. † A centrifugal pump, previously described in [2], circulates the liquid around the flow loop. To maintain a constant inlet temperature to the test section, heat is removed from the liquid as it passes through approximately 13 meters of 0. 32 cm i. d. copper tubing located in a heat exchanger reservoir of approximately 2. 5 liter capacity. The heat exchanger reservoir is continuously supplied with liquid helium from a storage dewar.

† Identification of any materials or their manufacturer by the National Bureau of Standards in no way implies a recommendation or endorsement by the Bureau. Furthermore, use of other trade names in this paper is for the sake of clarity and does not in any way imply a recommendation or endorsement by the Bureau.

* 1 atmosphere = $1. 013 \times 10^5 \text{ MN/m}^2$.

2. 1 Test Section

The test section is a 0. 213 cm i. d. x 20 cm long stainless steel tube with a wall thickness of 0. 016 cm. It is resistance heated along 10 cm of its length ($L/D = 50$). A stainless steel-pyrex seal located in the bottom of the loop provides electrical isolation of the test section. A wire wound preheater upstream of the test section allows variation of quality at the inlet of the tube. Accurate measurement of the current and potential drop across the two heaters is used in the calculation of heat flux. At the lowest power levels the uncertainty is less than 2%.

2. 2 Temperature Measurement

Outside tube wall temperatures are measured at ten points along the heated test section length with calibrated carbon resistance thermometers. A detailed sketch of a thermometer and the mounting scheme is shown in figure 2. † The thermometers are positioned one cm apart with the first thermometer located 0. 6 cm from the inlet. Inside wall temperatures are obtained by calculation of the temperature drop through the tube wall using the thermal conductivity of stainless steel given by equation (A1) in the appendix of reference [1]. Bulk fluid temperatures are measured at four points along the flow loop (upstream of preheater, upstream of test section and two measurements downstream of the test section) with germanium resistance thermometers. These thermometers are plotted with vacuum grease in copper wells which are soldered to the tube.

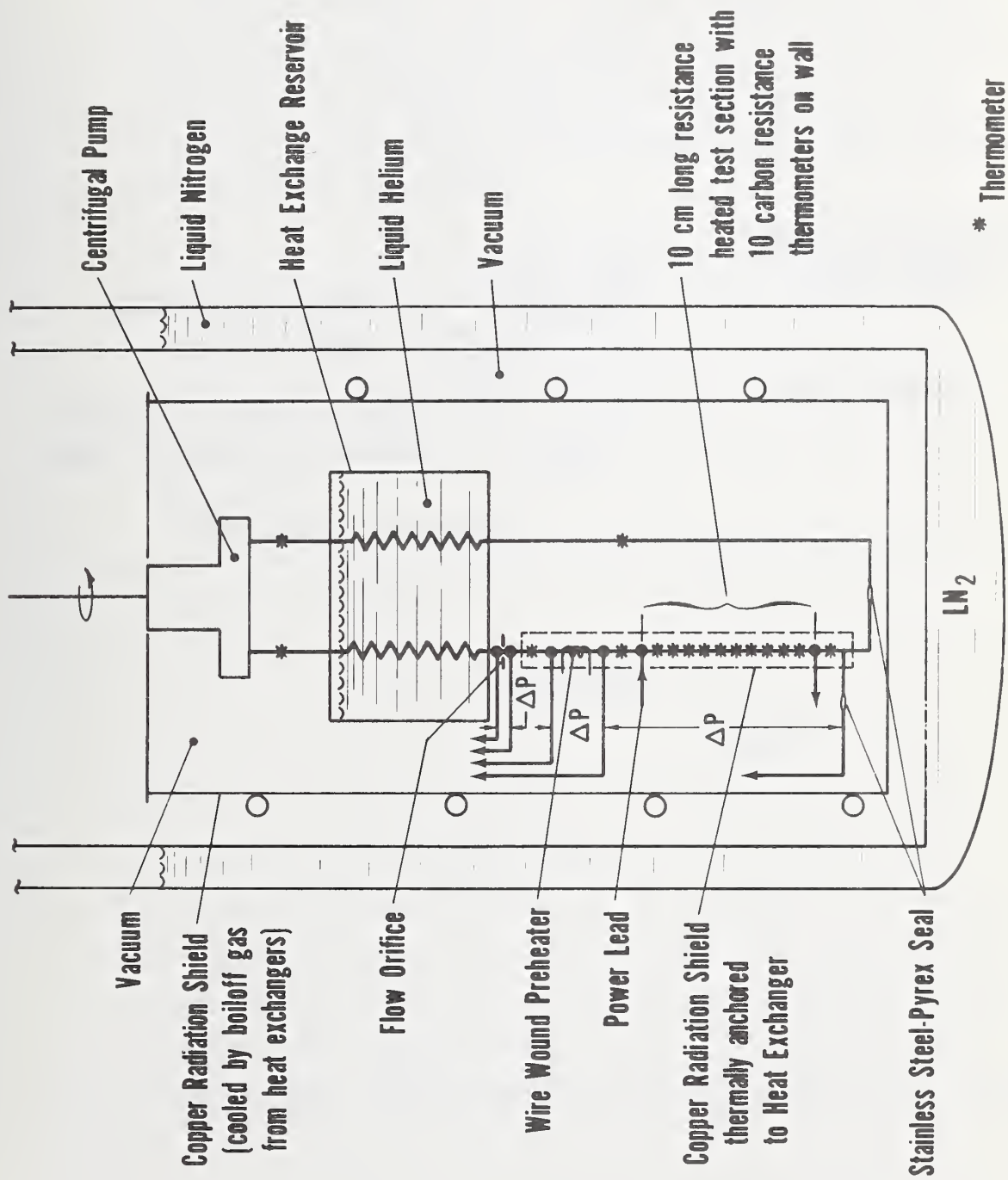


Figure 1. Schematic of the boiling heat transfer flow loop.

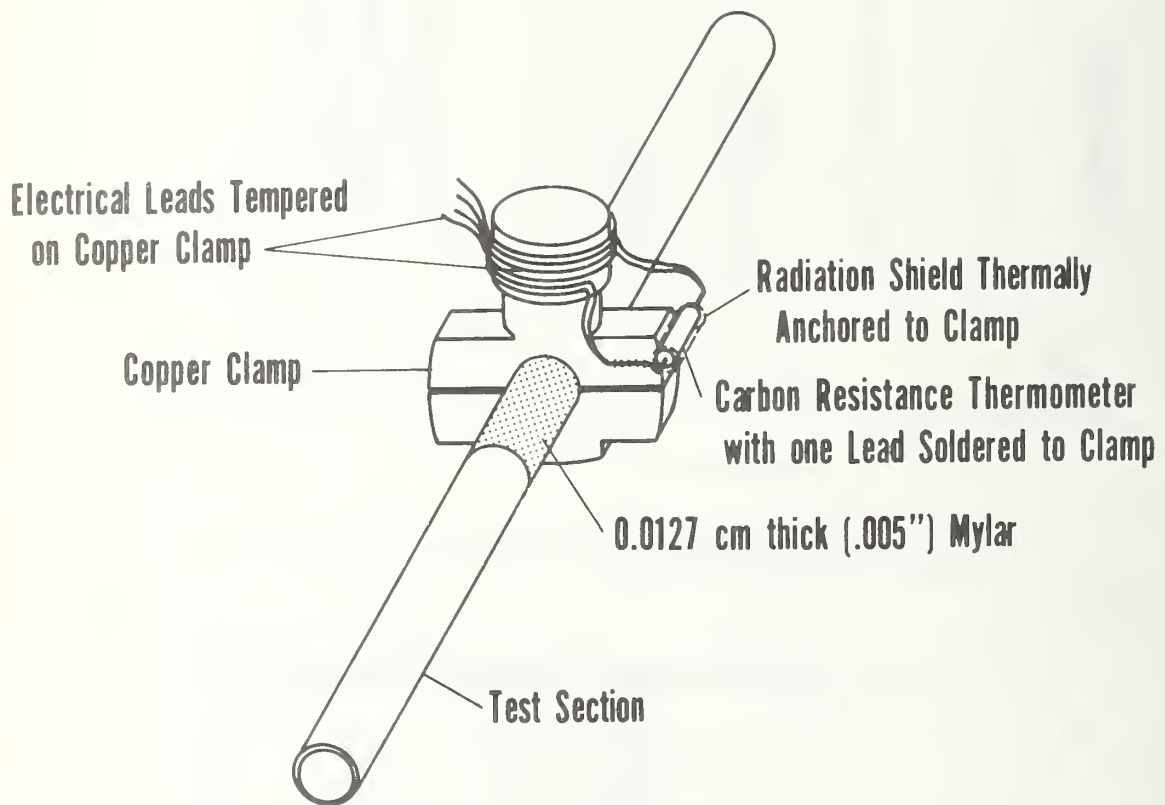


Figure 2. Sketch of mounting scheme for carbon resistance thermometers.

The carbon resistance thermometers and the germanium resistance thermometers used in this study were calibrated in a separate apparatus, over the range 4 - 20 K, against three germanium resistance thermometers (GT 1011, 1027 and 1024). These three germanium thermometers had been previously calibrated against NBS secondary standard germanium thermometers (GT 722 and 734).

In our calibration, over the range 4 - 9 K the agreement between GT 1011, 1027 and 1024 was within 0.01K for the worst case and was generally within 0.005 K. Above 9 K the agreement was within 0.05 K. An average value of the three germanium thermometer readings was taken to be the true temperature.

The calibration data for each thermometer were fitted with a curve of the form

$$\text{LOG } T = \sum A(N) \text{ LOG } R^N$$

with an rms percent error of 0.300 in temperature or less.

After a period of about six months, and after several intermittent thermal cycles from room temperature to helium temperature, three carbon thermometers and two germanium thermometers were removed from the experimental apparatus and dip tested in liquid helium (4.025 K) to check for a shift in calibration. The carbon resistors were within 0.1%, 1.1%,

and 1.2% in temperature of their original calibration while the germanium thermometers were within 0.3% and 0.5%. It should be noted that while this does not represent a calibration shift for the germanium thermometers, the error for two of the carbon resistors lies slightly outside of the 99% confidence limit of the original calibration (i. e. $3 \times$ rms percent error).

In the two-phase region, since the pressure drop across the test section was of the order of a few mm Hg for the data presented, the intermediate bulk temperatures were taken to be the saturation temperatures corresponding to the inlet static pressures. This approximation was within experimental error.

Periodic zero power runs were made to check consistency among the fourteen thermometers. Agreement between the four germanium resistance thermometers was within a few millidegrees while the carbon resistance thermometers showed a decreasing offset with time when compared to the germanium resistance thermometer readings. The time constant (of the order of hours) was too long for it to be practicable to wait. Since the time of each powered run and each zero power run was recorded, this well-defined offset was used to correct the carbon resistance thermometer readings. This correction also takes care of any shift in calibration of the carbon resistance thermometers. Extensive tests on the carbon resistance thermometers in a separate apparatus (with the thermometers mounted exactly the same as in the present study) showed that they are extremely sensitive to irradiation from high temperature sources. It is felt that although substantial effort was devoted to radiation shielding of the carbon thermometers, the

radiation could not be totally eliminated during the period that the entire apparatus approached temperature equilibrium. The estimated uncertainty in outside wall temperatures is at most 0.05 K. The error in the temperature difference between the inside wall and the bulk temperature is due to uncertainty in the thermal conductivity of the stainless steel wall, the wall thickness, and uncertainty in bulk temperature. This varies from 26% to 53% below the critical heat flux (see 3.1) to 0.3% above this transition.

2.3 Pressure and Flow Measurement

Provision was made to measure pressure drop across the flow orifice, preheater, and test section, and the static test section inlet pressure using calibrated pressure transducers and a static Bourdon tube pressure gauge accurate to 0.01 atm located outside the cryostat at room temperature. Test section pressure drop will be reported in a future report but was small, generally less than 7 mm Hg.

Since the fluid at the outlet of the preheater was slightly subcooled for the data presented here, a calorimetric method determined the flowrate. The calorimetric flowrate was also used to determine a discharge coefficient for the flow orifice so that the orifice may be used for flow measurement when calorimetric flow determination is not possible, i. e., two-phase out of the preheater. The discharge coefficient so obtained agrees well with that of an identical orifice section which was calibrated in a separate apparatus. The accuracy of the flow rate measurement has not yet been fully evaluated, but we believe the values based on calorimetry to be accurate to a few percent.

2.4 Extraneous Heat Exchange

To minimize heat leak from room temperature to the test section by conduction, all electrical leads and the thin walled, 0.317 cm diam. stainless steel pressure transmission lines are thermally anchored to the outside copper surface of the liquid helium heat exchanger. A length of multifilament niobium-titanium superconducting wire is used for power leads between the heat exchanger and the test section and between the heat exchanger and the preheater. The small diameter and low thermal conductivity of this wire further minimizes heat leak due to conduction and joule heating in the leads is eliminated. Error in heat flux due to axial conduction from the ends is less than 2% for the worst condition. Extraneous heat to and from the test section is therefore considered negligible. Boil-off from the liquid helium heat exchanger is routed through coils soldered to the pump housing and the radiation shield. This arrangement minimizes heat leak from room temperature via conduction along the pump housing and provides a low temperature radiation shield around the flow loop. The test section portion is further protected from radiation by a copper shield thermally anchored to the heat exchanger. The evacuated copper enclosure (vacuum less than 10^{-7} mm Hg) which is submerged in a bath of liquid nitrogen provides first stage radiation shielding from room temperature.

2.5 Experimental Measurement

For a fixed system pressure, pump speed and quality at the inlet of the test section, the power to the test section was varied over a range from zero to that at which a discontinuous

rise in the wall temperature occurred at the outlet end of the test section (critical heat flux). For some of the runs this heat flux was exceeded causing the discontinuity in wall temperature to move up the test section. After a change in test section power, thermometer voltages stabilized generally within a few seconds and were recorded by a digital voltmeter and automatically punched on paper tape together with all other pertinent voltages and run information.

Since the flow loop is a closed system, as power was applied it was necessary to vent the system to maintain a constant test pressure, and conversely a decrease in power applied required adding and condensing gas in the loop to maintain the pressure.

This procedure was repeated for different pump speeds, inlet quality and pressure.

During a measurement the temperatures and pressure were stable to within their accuracy prior to a transition in the heat transfer mechanism (critical heat flux exceeded). When a transition occurred, it was accompanied by fluctuations in temperature (for the wall stations in the transition region) of a rather random frequency, and an amplitude of the order of 0.5 K. Oscillations in pressure were not noticeable but this was at least partly accountable for, the pressure transmission line being heavily damped.

One of the goals of the present study is to establish the repeatability of a measurement in the form, say, of the spread in wall temperatures which can be expected when the flowrate, pressure and inlet enthalpy are specified. To date, we do not

have sufficient information to establish a day-to-day variability, but we do have a few figures for the variability observed during the course of a day's running. Below the critical heat flux this variability is generally of the order of a few percent of the excess of wall temperature over bulk temperature, with a worst value observed of 11%. Above the transition, we do not have sufficient data at this time to estimate the variability.

3. HEAT TRANSFER RESULTS

3.1 Wall Temperature Profiles

Temperature profiles along the wall for subcritical helium are shown in figures 3 through 10 for pressures from 1.1 to 2.1 atm and mass velocities from 4.8 to 63.6 g/cm². A typical profile is extremely flat up to some point at which a sharp rise is observed for the higher heat fluxes. This we identify, with reference to a vast body of literature on boiling heat transfer, as indicating a hydrodynamic transition from wetted-wall, e. g. , nucleate boiling, to dry-wall, e. g. , film boiling, heat transfer. Thus, at a particular point along the test section there is a critical heat flux above which the wall temperature rises quite steeply with heat flux.

Below the critical heat flux, heat transfer is very good as evidenced by the wall temperatures being nowhere more than 0.3 K above the bulk fluid temperature. Indeed this behavior is strongly reminiscent of boiling heat transfer without forced convection, i. e. , pool boiling. In figures 11 and 12 we plot the heat flux q against the difference between the wall and bulk fluid temperatures for the first and last wall thermometers

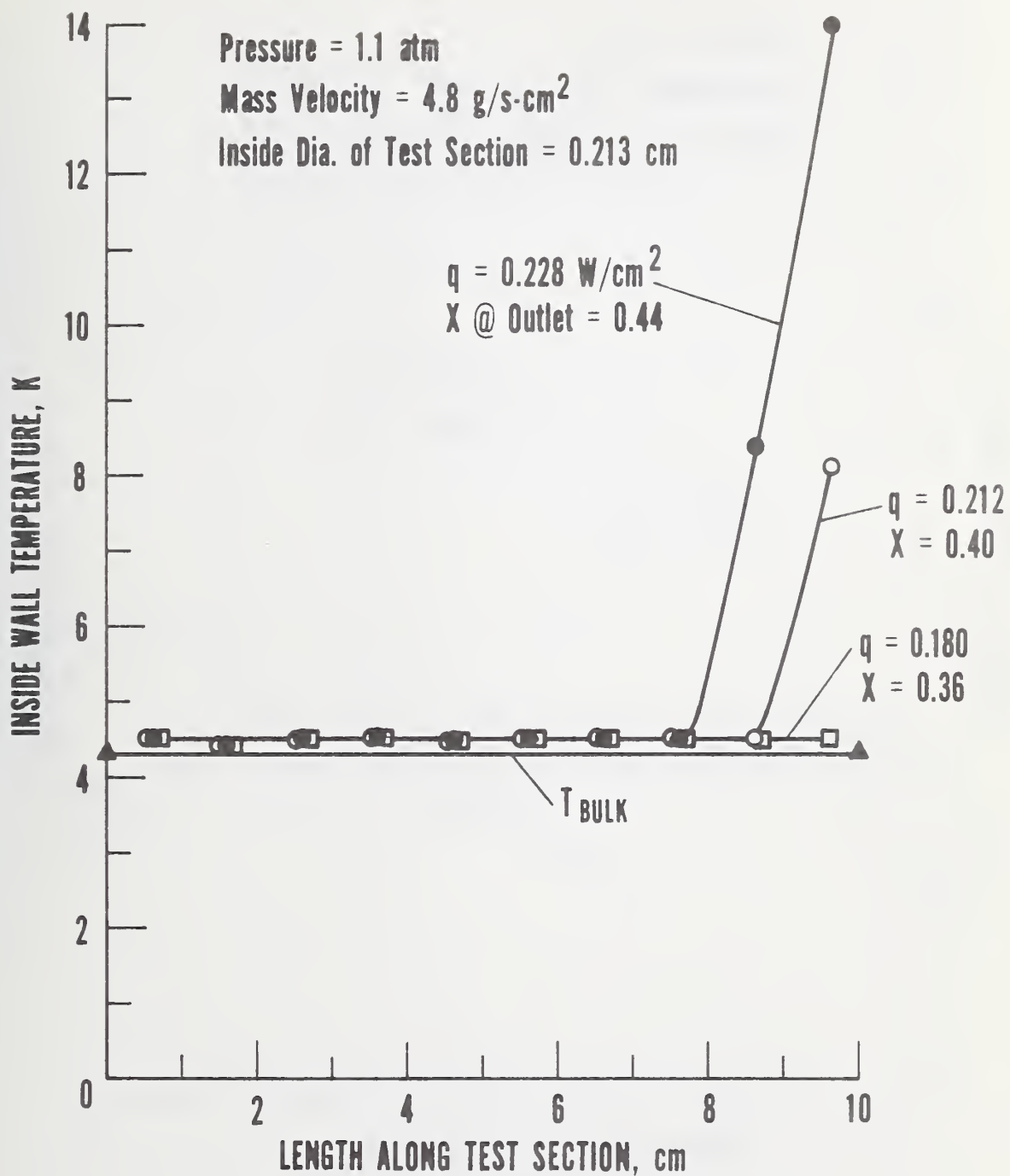


Figure 3. Wall temperature profile for test section.

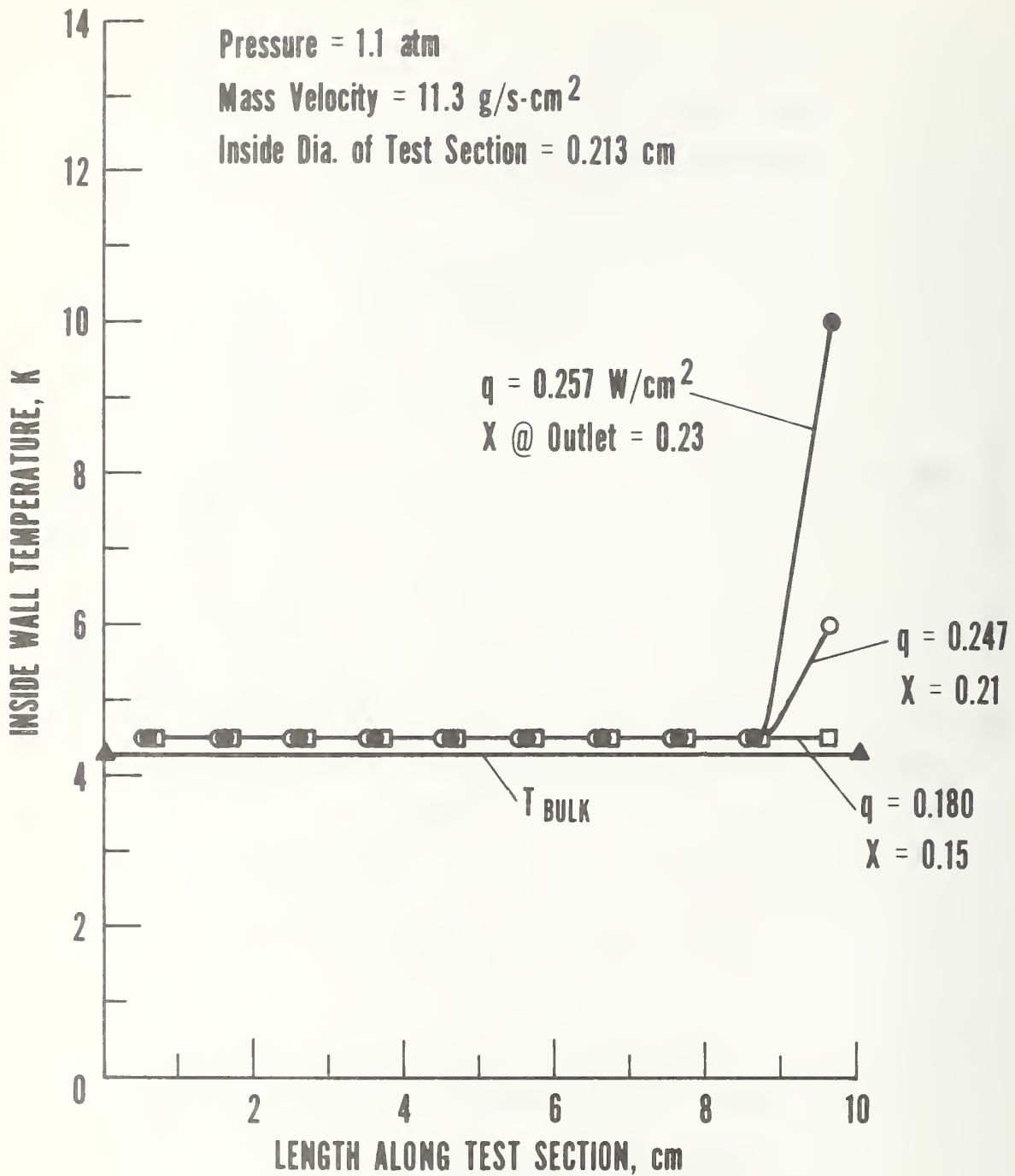


Figure 4. Wall temperature profile for test section.

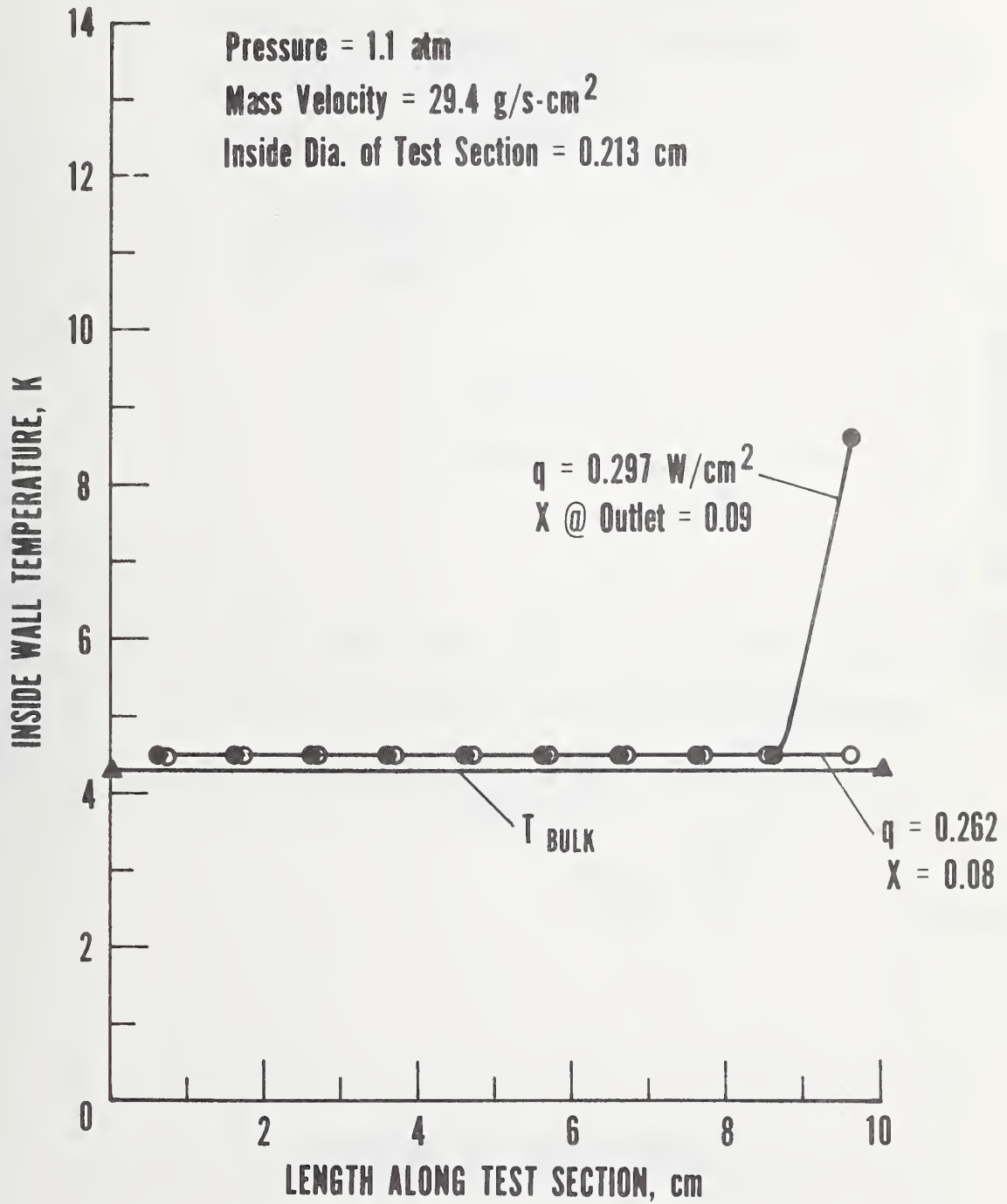


Figure 5. Wall temperature profile for test section.

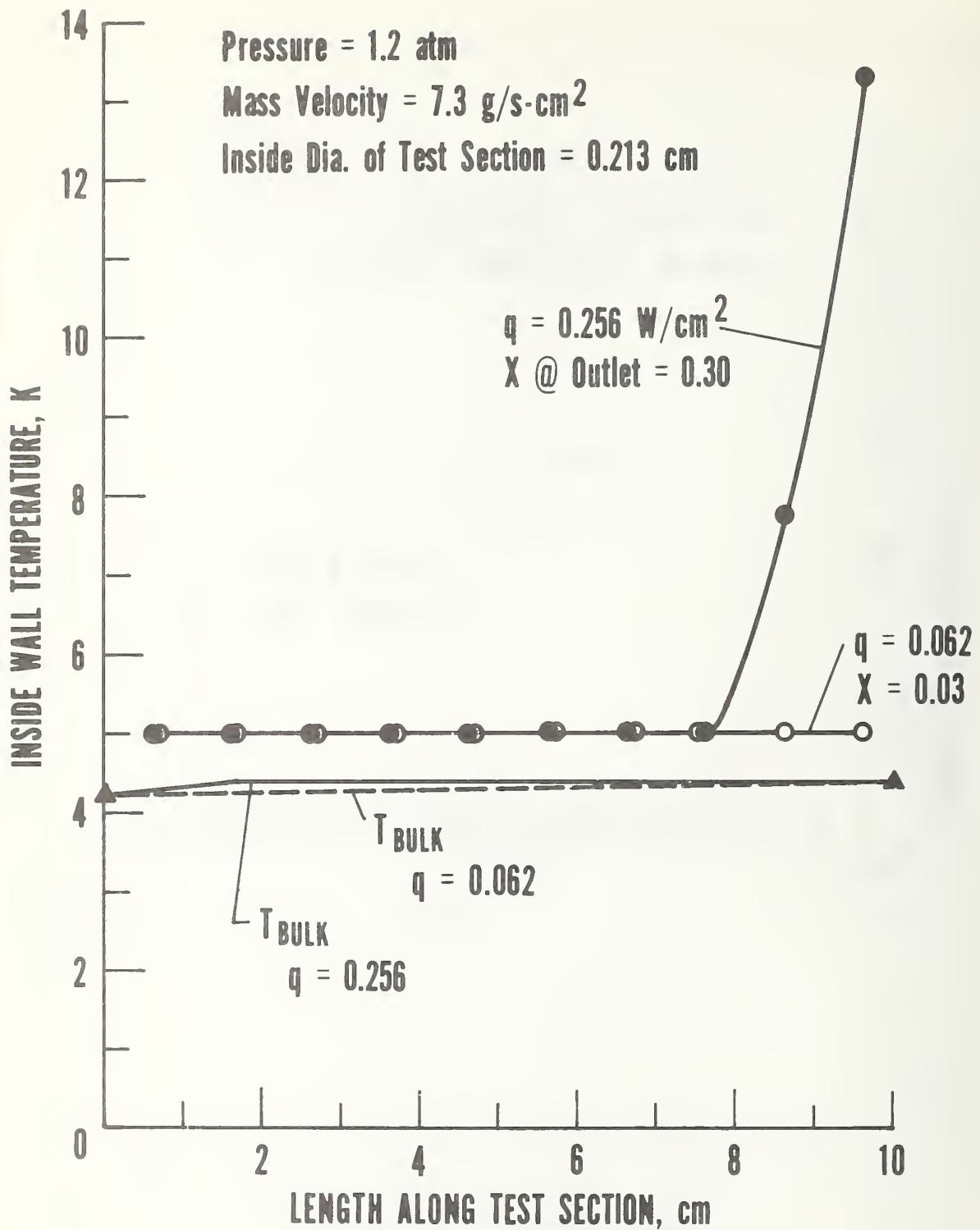


Figure 6. Wall temperature profile for test section.

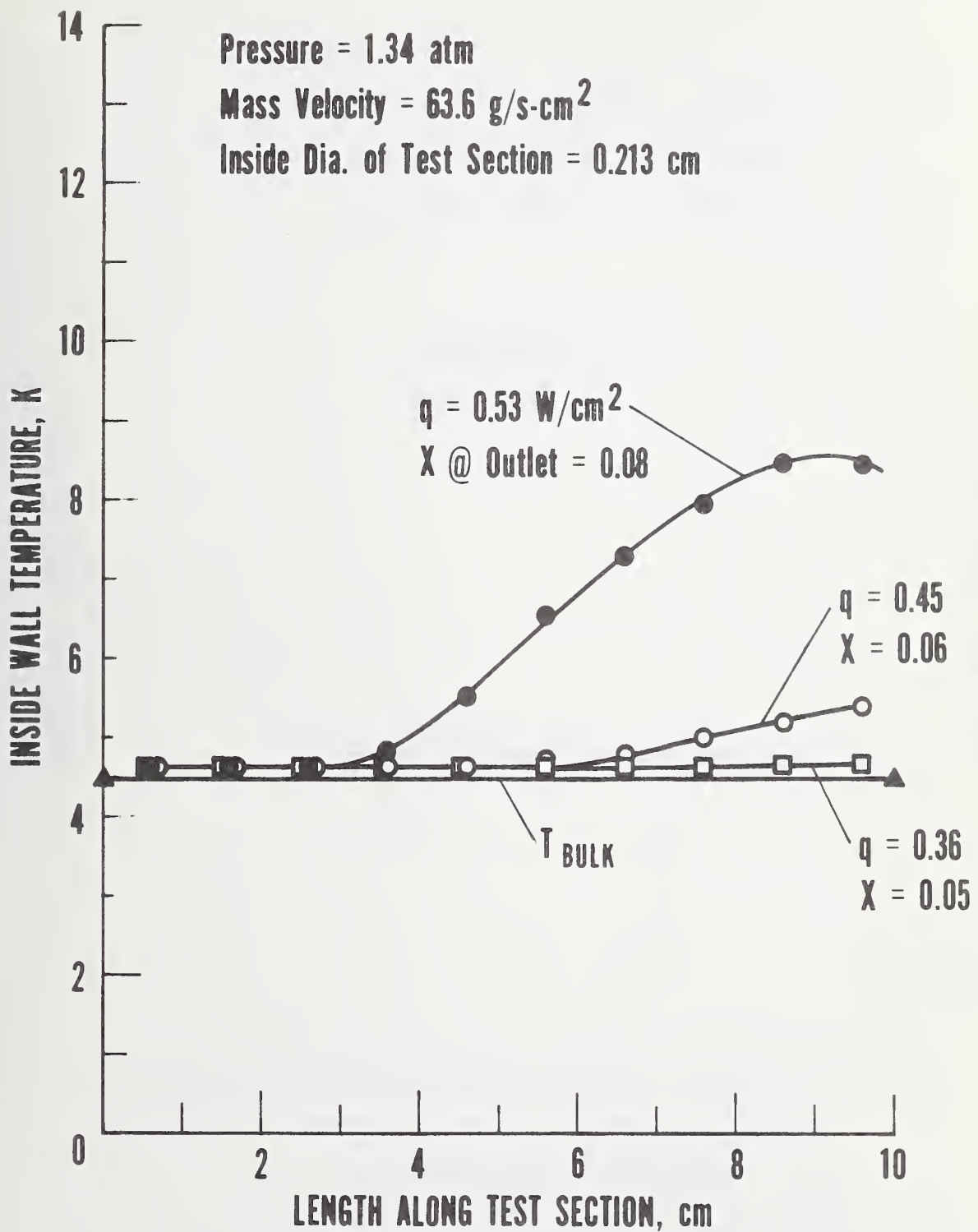


Figure 7. Wall temperature profile for test section.

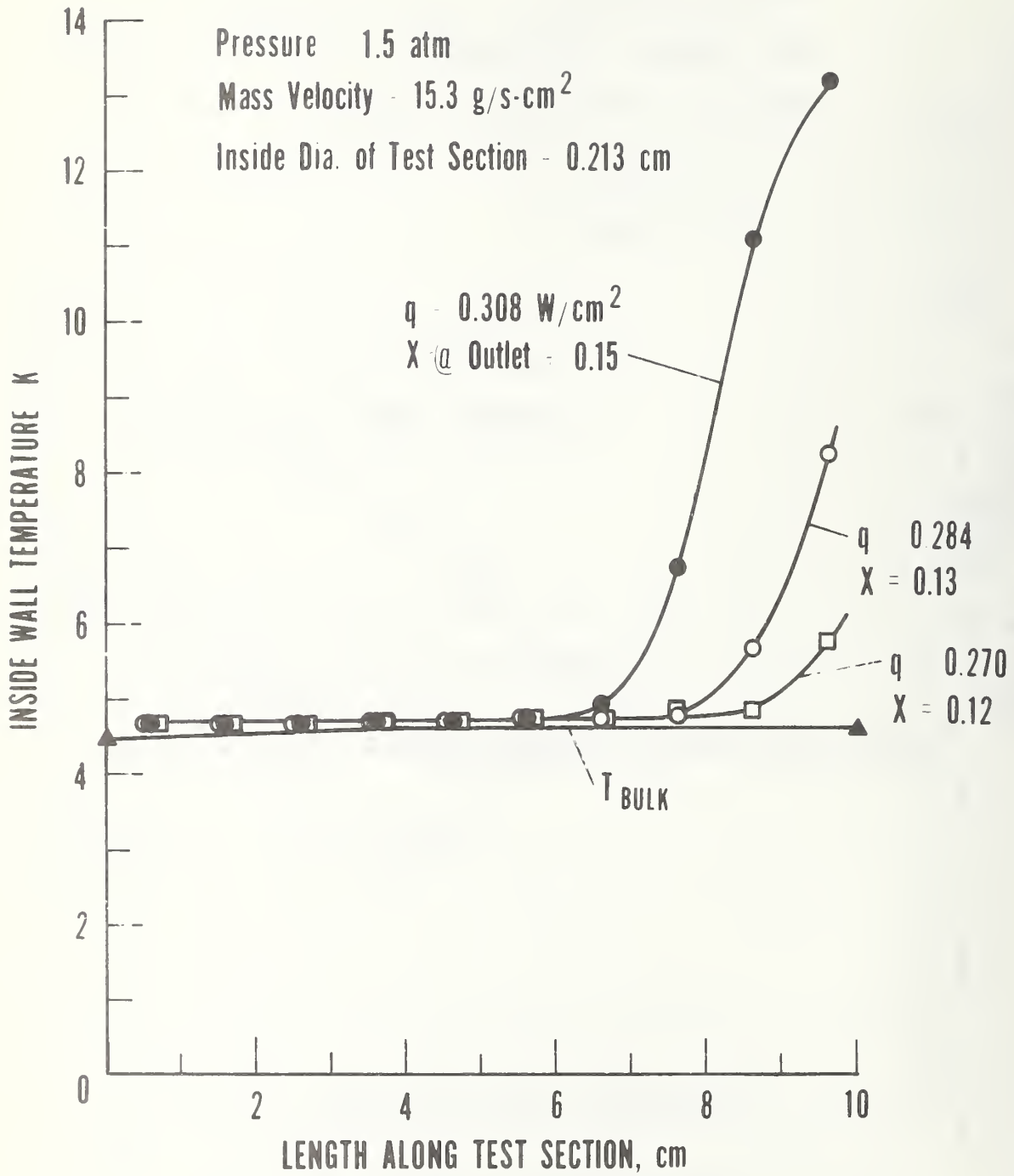


Figure 8. Wall temperature profile for test section.

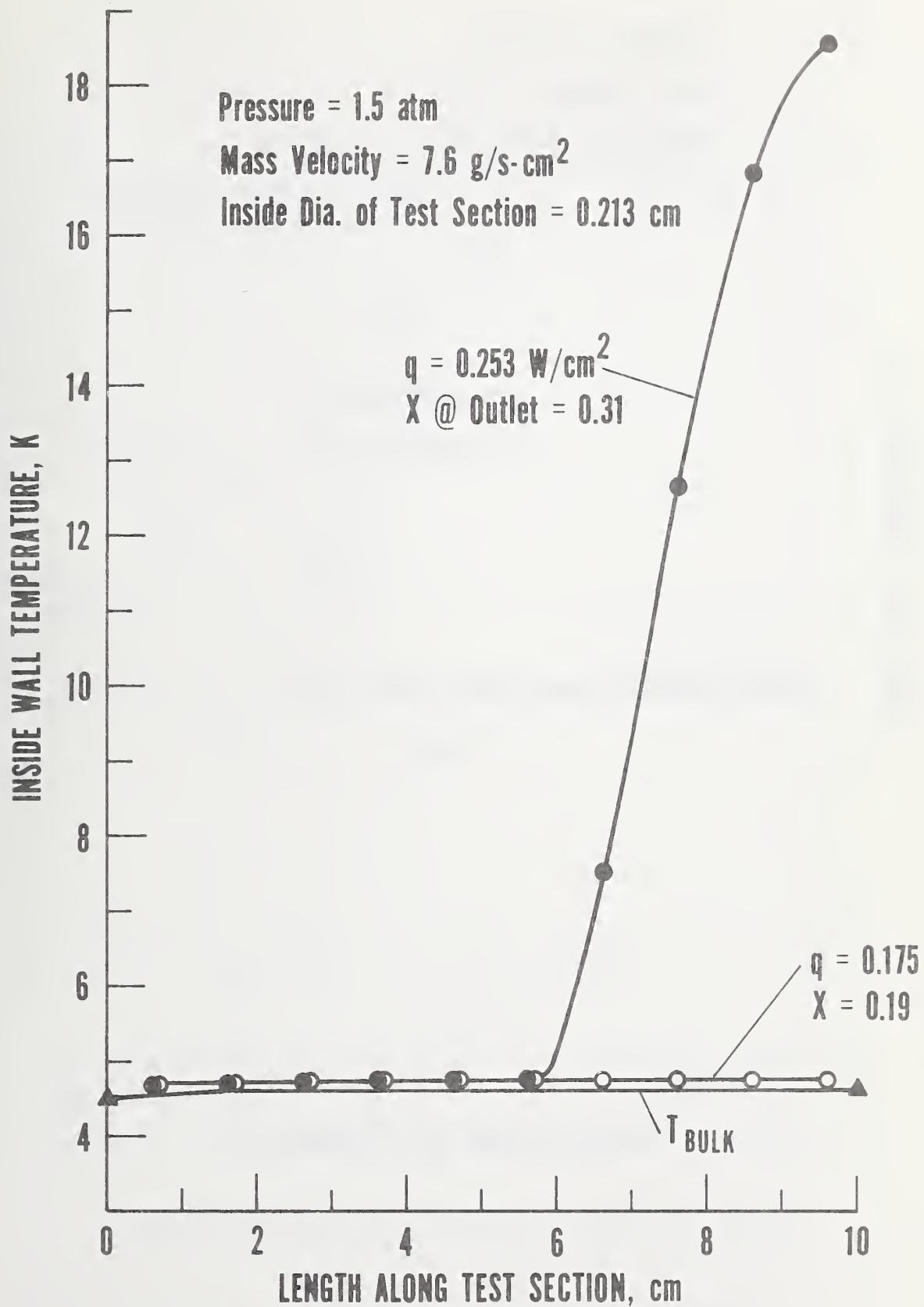


Figure 9. Wall temperature profile for test section.

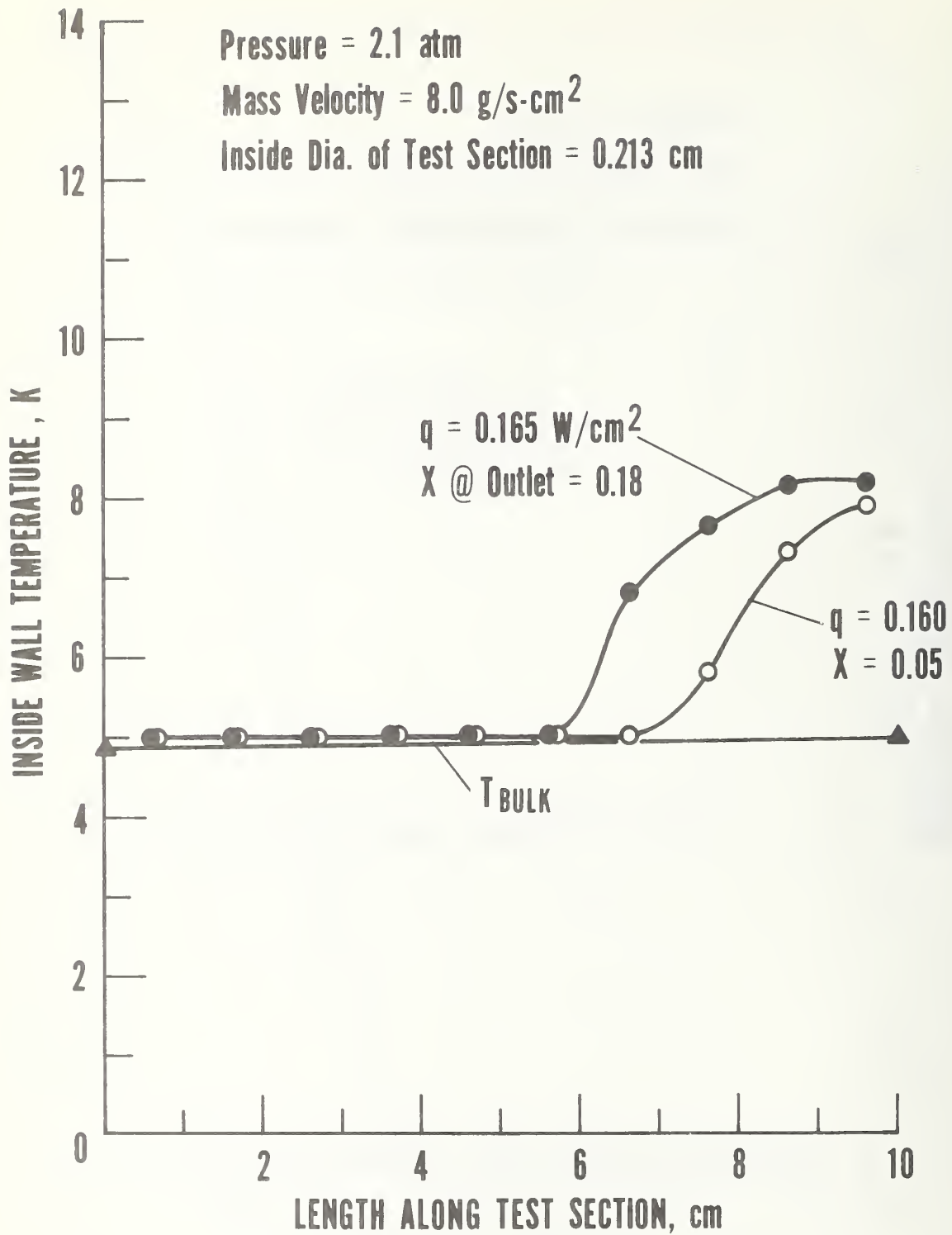


Figure 10. Wall temperature profile for test section.

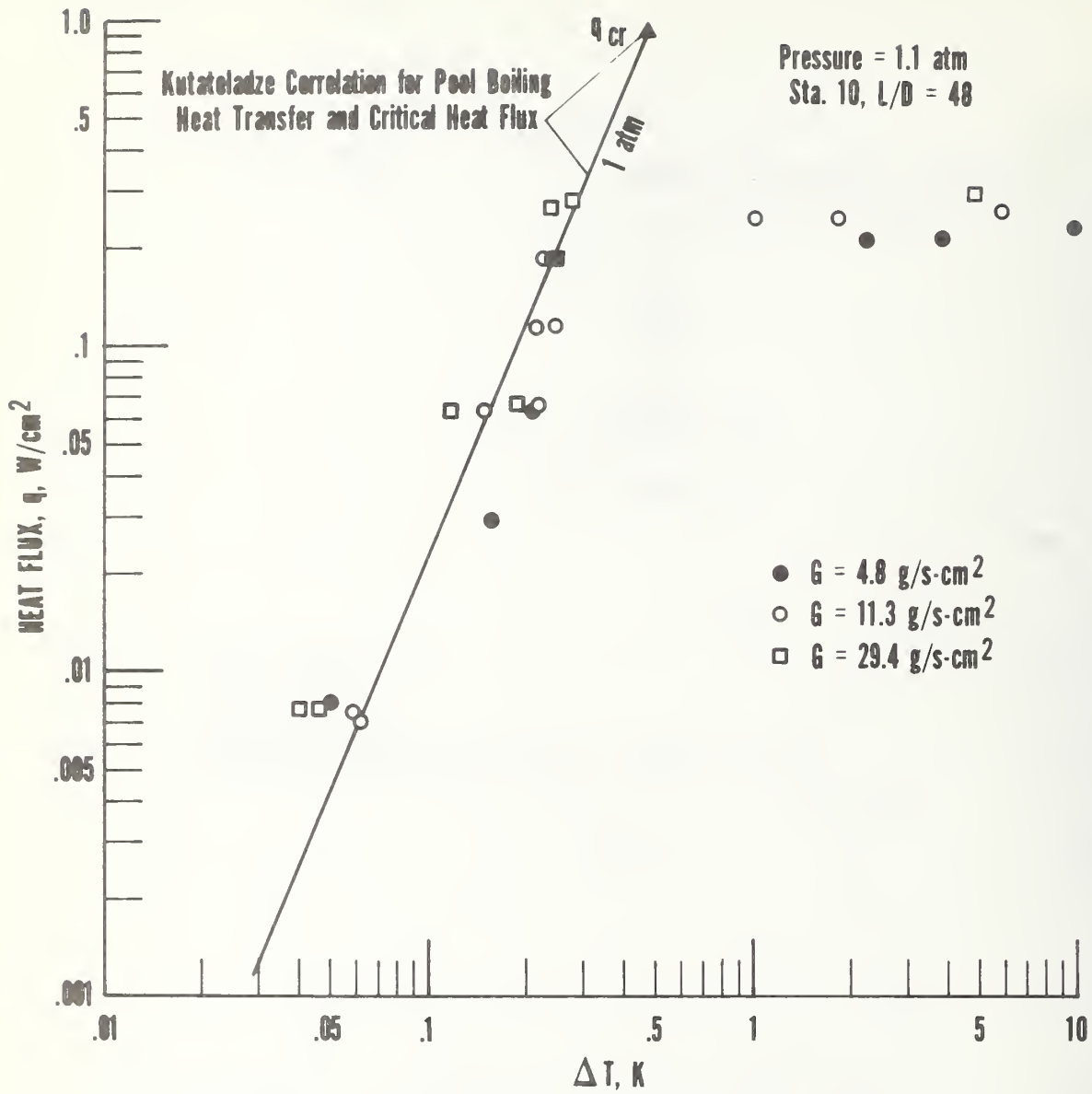


Figure 12. Heat flux vs temperature difference for station 10.

respectively. These are at 3 and 48 tube diameters respectively from the commencement of the heated length of the test section. We have also plotted as a solid line the nucleate pool boiling correlation of Kutateladze [7] and indicated at its upper extremity the critical heat flux for pool boiling given by a second correlation due to Kutateladze [7]. As shown for example by Brentari and Smith [8] these correlations give a good average representation of nucleate pool boiling data for cryogenic fluids. The present data for forced convection heat transfer are represented by the first of these correlations below the critical heat flux as well as any given set of pool boiling data, which are notorious for their sensitivity to the precise nature and preparation of the boiling surface, as well as its heating history (a strong hysteresis effect is often observed). We conclude that forced convection has had very little effect on the rate of heat transfer at heat fluxes below the critical and that the boiling mechanism itself is the primary determinant.

In figure 13 a wall temperature profile for subcritical helium is compared with one for supercritical helium flowing at approximately the same mass velocity and the same applied heat flux. This comparison illustrates well the essential difference between two-phase and single-phase heat transfer; provided transition is not allowed to occur the boiling phenomenon is extremely effective in holding down the wall temperature. However, we draw attention to the last wall temperature which, in the subcritical profile shows a slight increase in temperature indicative of the onset of transition to dry-wall heat transfer. This is seen in figure 9 in a more highly developed stage

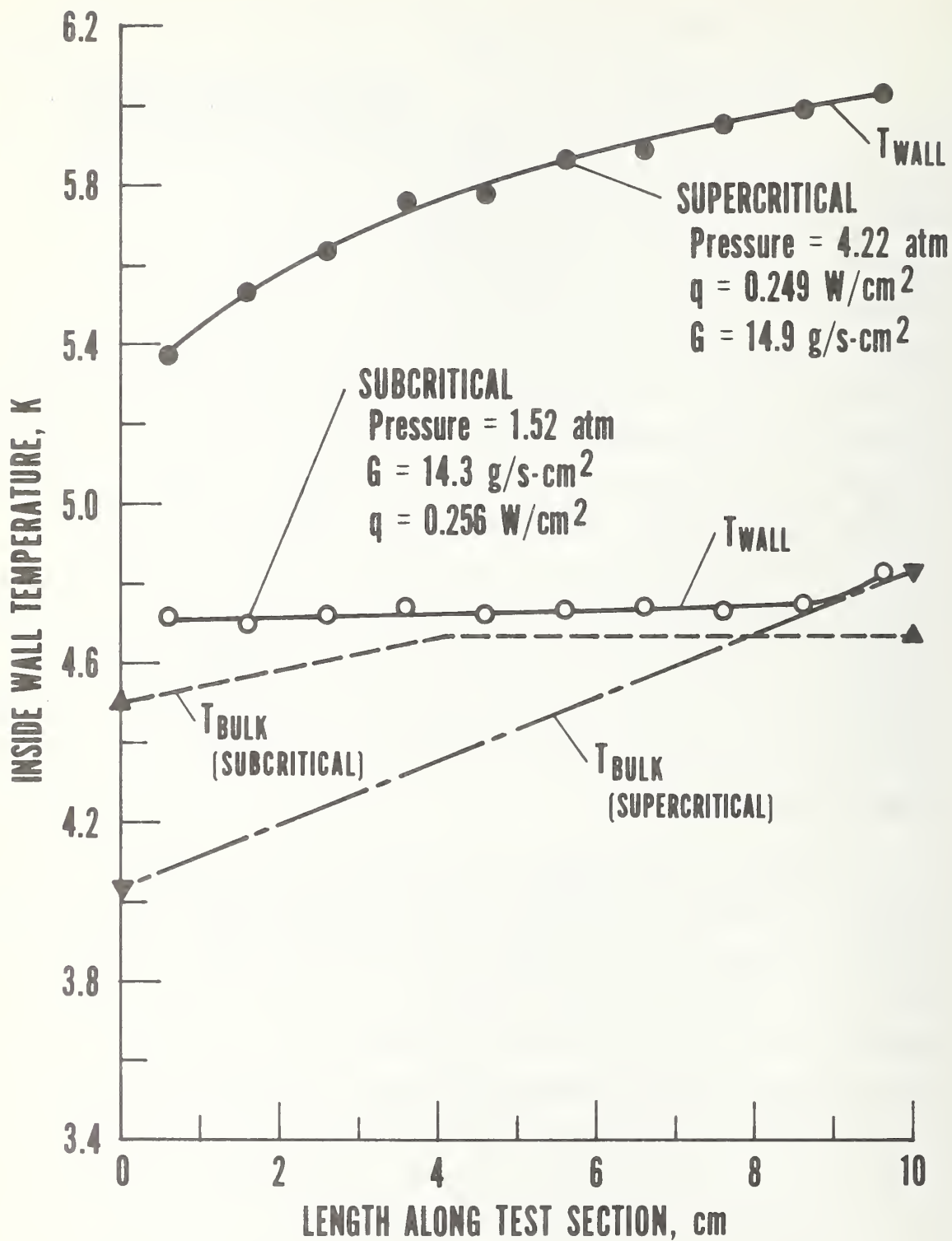


Figure 13. Comparison of subcritical and supercritical wall temperature profiles under similar mass velocity and heat flux conditions.

at higher heat fluxes. The comparison between heat transfer in these two pressure regions is discussed further in 3.3 below.

3.2 Critical Heat Flux

Beyond the critical heat flux the wall temperatures may rise to quite unacceptable heights, from the point of view of the cooling of superconductors, as is clearly seen from figures 3 through 10 and figure 12. It is therefore of great importance to be able to predict the conditions under which the transition from wetted-wall to dry-wall heat transfer takes place. In fact, from this point of view it is almost the only consideration of importance until the flow rates become very high, because the wall temperature rises observed in the wetted-wall region are so small as to be of no concern, and in the dry-wall region they are generally so large as to preclude this region from consideration. However, at high flow rates, as seen in figure 7, the wall temperature excursion appears to have reached a limit which may be of some practical value in superconducting technology. Figure 7 gives data for the highest flow rates obtained in this study, and thus it appears that at very high flow rates the transition may be kept within useful bounds.

One of the ultimate goals of this program will be to provide a means of predicting the transition, that is: given the state of the fluid at entry to the heated section, i. e. , enthalpy and pressure, the flow rate and the heat flux, we wish to know at what position downstream the transition will occur. Alternatively, given the state and flow rate, we wish to know the heat

flux--the critical heat flux--at which the transition will occur at a certain position. Considerably more data than are so far available from this study will be required. For the present, however, we shall confine our attention to identifying trends.

The first and most obvious trend is that, for a given pressure and mass velocity, the critical heat flux is a function of distance from the inlet to the heated section. In experiments on heat transfer to subcritical helium under conditions of natural convection, Johannes and Mollard found that most of their data could be represented by a single curve when the critical heat flux was plotted against the distance from the inlet to the heated section in diameters (the hydraulic or equivalent diameter D_e is used for rectangular cross sections where $D_e = 4 \times \text{cross-sectional area} / \text{heated perimeter}$). Figure 14 shows this plot with our data points superimposed. The short channel data of James, et al., the long channel data of Keilin, et al., and the data of Jergel and Stevenson are also included. Those of Jergel and Stevenson were for a long channel with a small heater at the inlet. These and the data of Keilin, et al., were for forced flow.

The trend shown by Johannes and Mollard is confirmed, but now also an enhancement with increasing mass velocity is observed. The point at 2.1 atm (reduced pressure 0.93) being lower even than the curve representing the data of Johannes and Mollard is not surprising and illustrates a fact familiar from pool boiling, namely, that the critical flux goes to zero at the critical pressure in accord with Kutateladze's critical heat flux correlation.

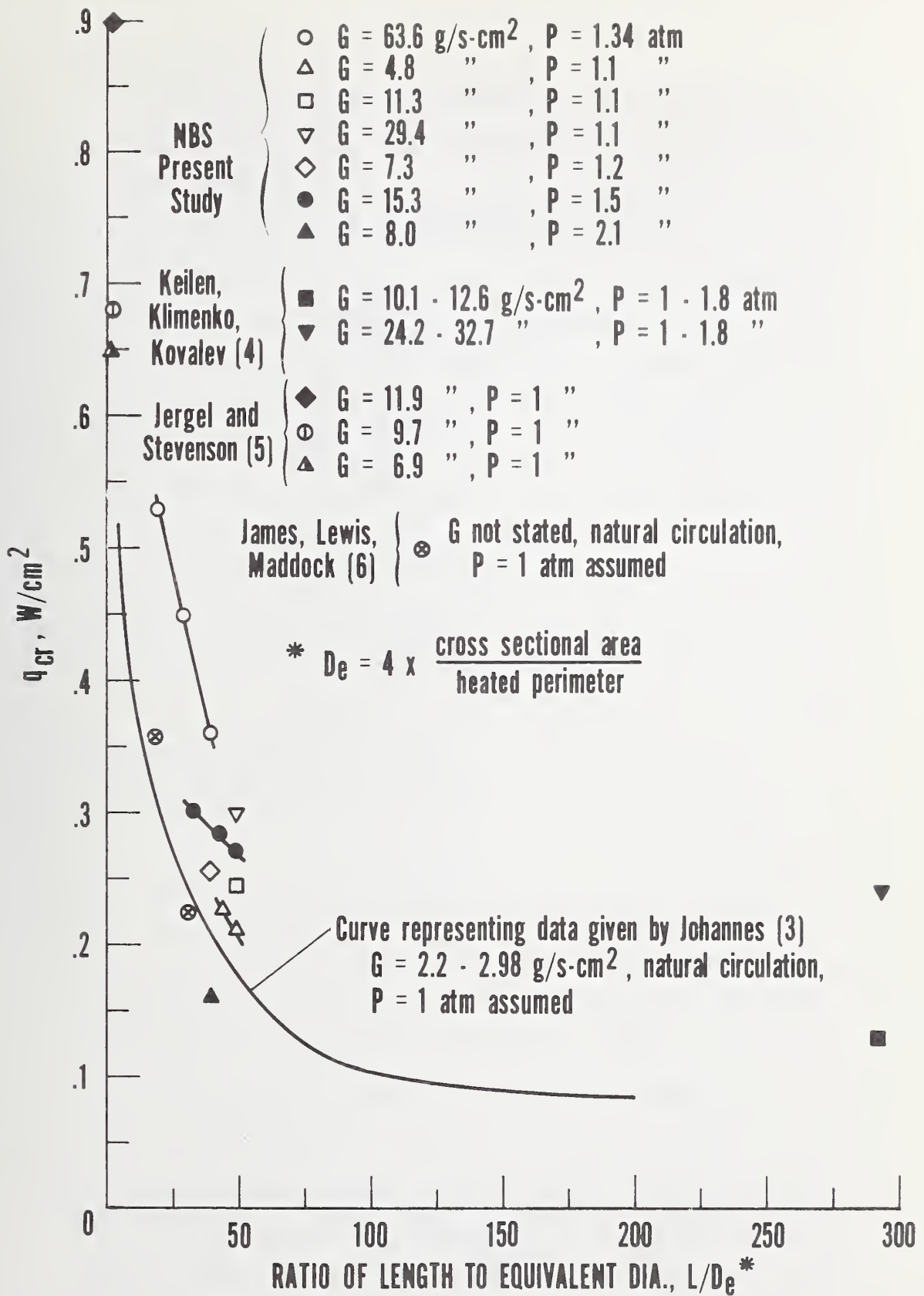


Figure 14. Critical heat flux as a function of length to diameter ratio with pressure and mass velocity as parameters.

It is hardly necessary to point out that if the conditions leading to transition in forced convection heat transfer were the same as those for pool boiling, then the entire tube would undergo transition at the same heat flux contrary to figure 14. It is therefore necessary, in order to properly account for transition in forced convection heat transfer, to look for either purely local conditions that change with L/D or to relate the hydrodynamic condition at a given L/D to the entire set of conditions upstream. In the search for a local explanation it is tempting to plot transition data against the local mass fraction of vapor (quality) at a fixed L/D . Since the heat transfer coefficient ($h = q/\Delta T$) is a sensitive indicator of hydrodynamic conditions, we have plotted this in figure 15 against quality at $L/D = 48$. Transition is strongly indicated by a pronounced maximum. We note the following:

- i. As with the critical heat flux, the critical heat transfer coefficient increases with mass velocity for a given pressure.
- ii. The transition occurs at decreasing qualities for increasing mass velocity for a given pressure.
- iii. For a given quality the heat transfer coefficient generally increases with mass velocity below the transition,
- iv. The higher the quality at which transition occurs the lower the corresponding heat transfer coefficient.
- v. For the pressures plotted in figure 15, increasing pressure has the same effect as increasing mass velocity. Unfortunately we do not have sufficient data

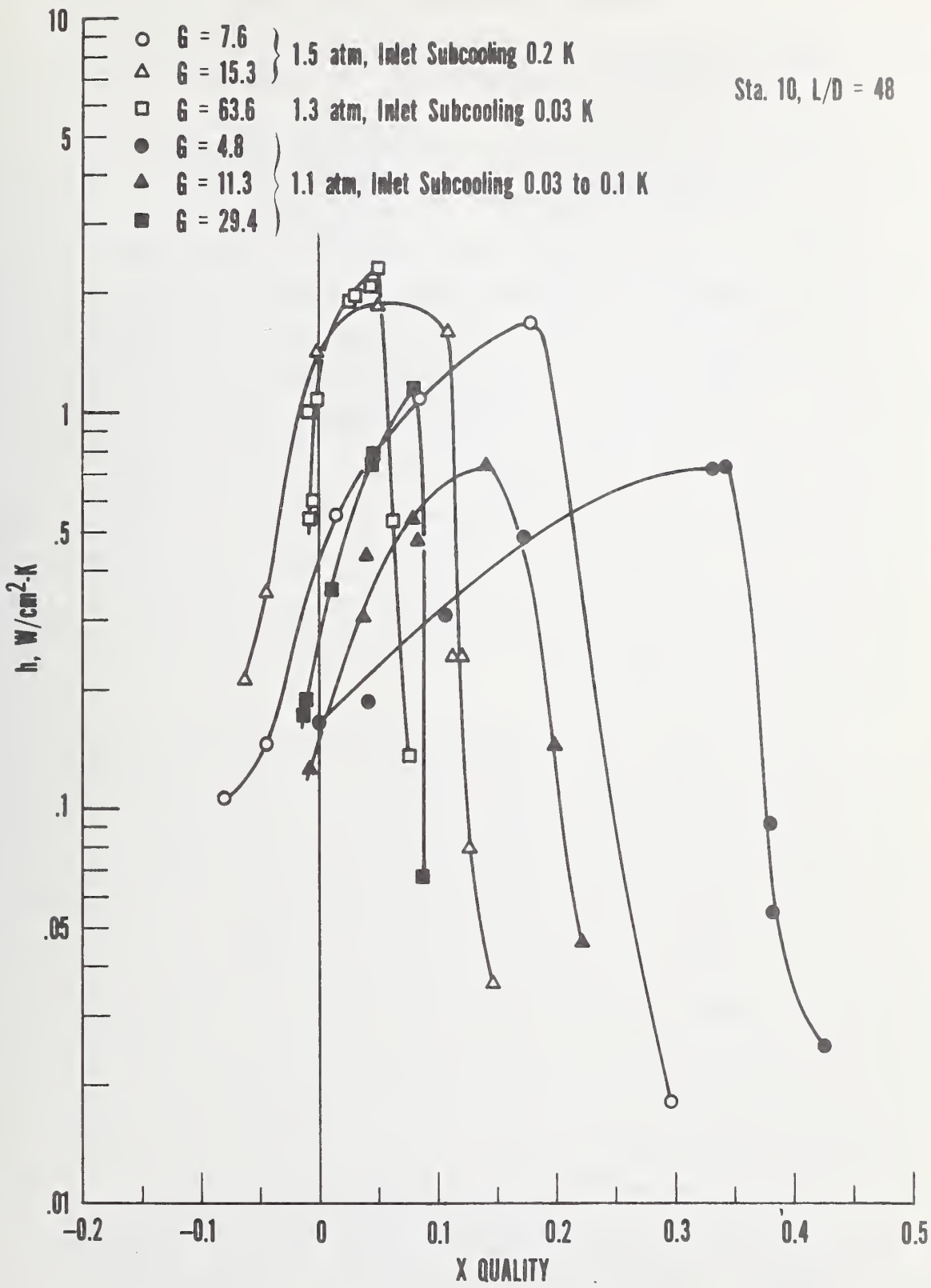


Figure 15. Heat transfer coefficient as a function of quality with mass velocity and pressure as parameters.

at 2.1 atm to be able to generalize this observation to near-critical pressures.

- vi. In all cases transition occurs while a substantial fraction of liquid remains.

It is clear that successful correlation of transition observations presents a considerable challenge; there are at least six interdependent variables involved apart from orientation effects. These are the critical heat flux, mass velocity, quality, pressure, diameter, and position along the heated tube or channel. We know, however, that this correlation must reduce to that of Kutateladze at low mass flow rates, for then the transition can be understood as a critical ratio between inertial, interfacial and buoyancy forces, which was the basis of that correlation. The development of a suitable correlation will be left to a subsequent phase of this work.

A rather interesting comparison can be made for the present transition results and those of Keilin, et al., for similar mass velocities and pressures. These authors report heat transfer coefficients in flat horizontal coils of copper tubing of 0.45 mm inside diameter at $L/D = 278$. In figure 16 the comparison is made with our data at similar mass velocities. The significant difference is in the quality at which transition apparently takes place. The heat transfer coefficient is also lower in accordance with trend iv noted above. Altogether, the transition observed by Keilin, et al., is much weaker than ours; we find from their report that their wall temperatures were nowhere more than 1 K above bulk fluid temperature even beyond the transition. It appears that the conditions of transition at

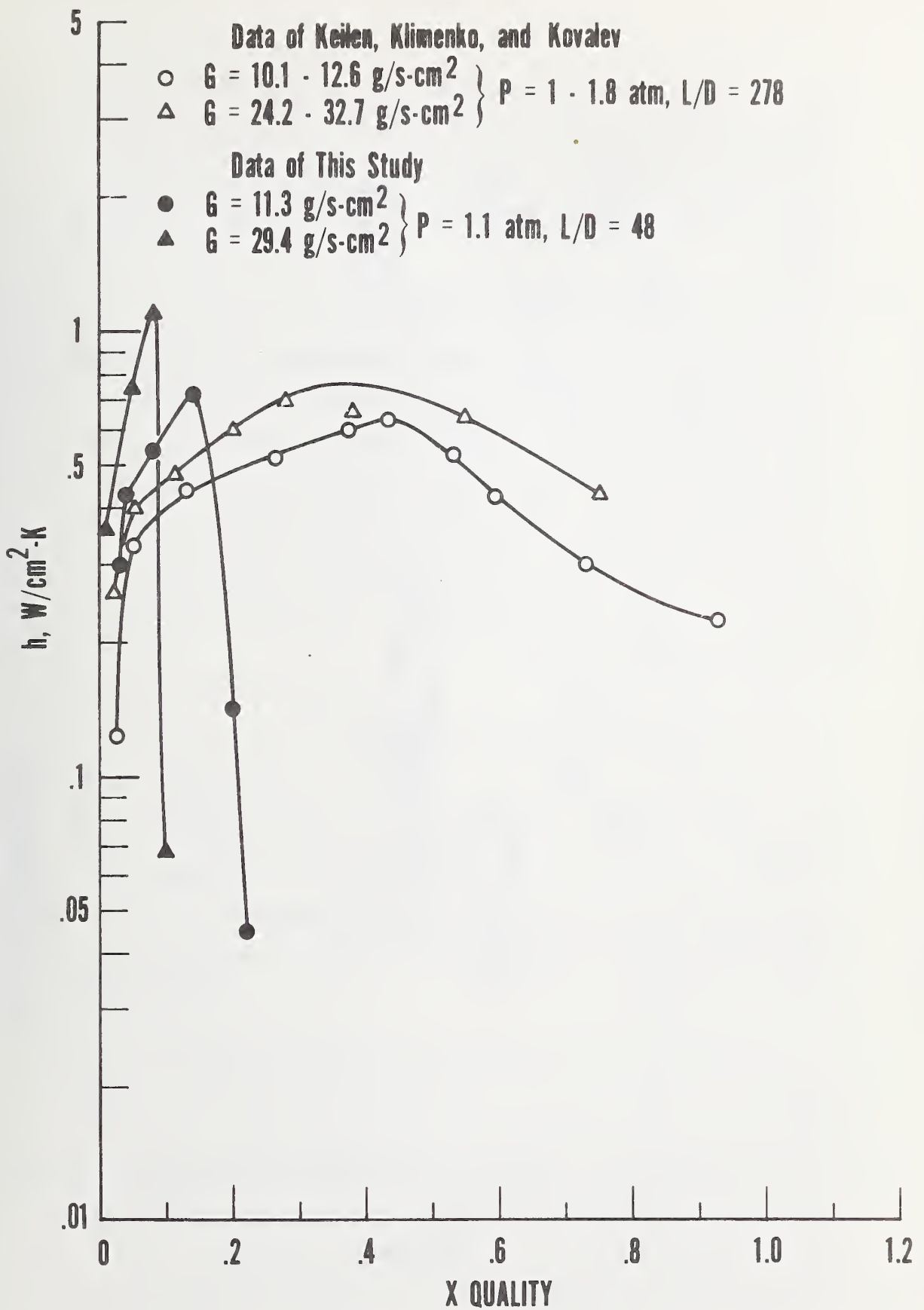


Figure 16. Heat transfer coefficient as a function of quality (comparison of this study's data with that of reference 4).

$L/D = 278$ are much different from $L/D = 48$. There is much more vapor present; therefore it must travel at higher velocity and the heat transfer coefficient after transition is not in such contrast with that before transition, which is the case in our results.

3.3 Comparison of Modes of Heat Transfer

In figure 17 the present results of heat flux q as a function of wall temperature rise ΔT are plotted for $L/D = 48$ for comparison with other modes of heat transfer. We have included calculated values of the nucleate pool boiling correlations of Kutateladze mentioned above and calculated values of q vs. ΔT for supercritical helium heat transfer at 3 atm and at Reynolds numbers of 10^4 , 10^5 and 10^6 . These were computed from the correlation

$$Nu = 0.0259 Re^{0.8} Pr^{0.4} \left(\frac{T_W}{T_B} \right)^{-0.716}$$

developed in reference [1] which represented the data of that reference ($L/D = 20$ and 40) with an rms percent deviation of 8.5%. Supercritical data obtained in the present work are represented by this equation to within 10% for most points for which $L/D > 20$.

We conclude from this comparison that for heat fluxes between 0.01 and 0.3 W/cm^2 subcritical pressures are preferable to supercritical pressures for equivalent mass velocities in forced convection. Above these heat fluxes, for the data presented here supercritical heat transfer is superior to subcritical, which is now in a dry-wall regime and shows very steep temperature rise for a small heat flux increment.

Sta. 10, L/D = 48
 Tube I.D. = 0.21 cm

Forced Convection Boiling Data

- $G = 4.8 \text{ g/s}\cdot\text{cm}^2$ } $P = 1.1 \text{ atm}$
- △ $G = 11.3 \text{ "}$ } $P = 1.1 \text{ atm}$
- $G = 29.4 \text{ "}$ } $P = 1.1 \text{ atm}$
- $G = 7.6 \text{ "}$ } $P = 1.5 \text{ atm}$
- ▲ $G = 15.3 \text{ "}$ } $P = 1.5 \text{ atm}$
- $G = 63.6 \text{ "}$ } $P = 1.3 \text{ atm}$

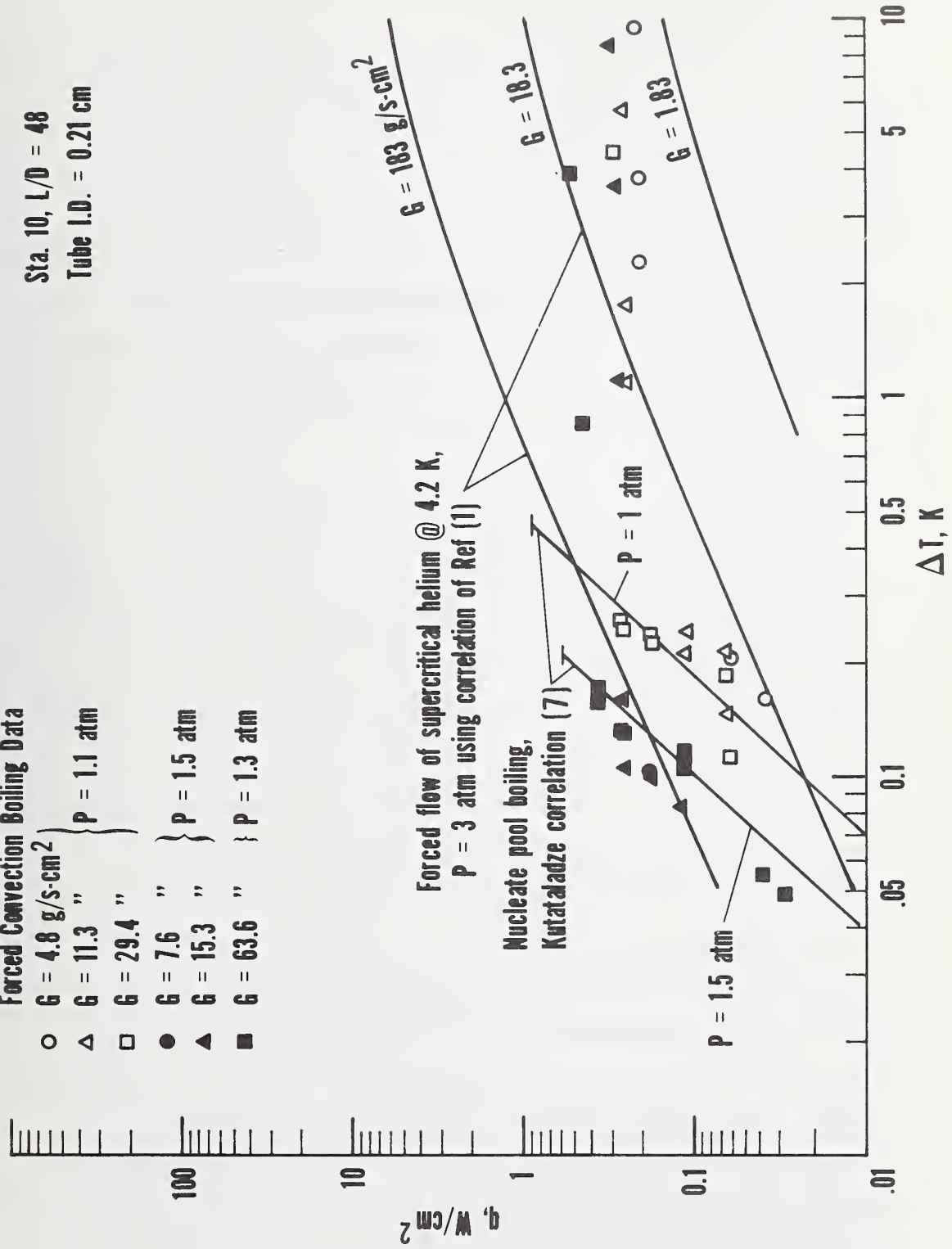


Figure 17. Comparison of modes of helium heat transfer.

4. PERFORMANCE OF CENTRIFUGAL PUMP WHILE CIRCULATING LIQUID HELIUM

During the performance of the heat transfer experiments there was no evidence of vapor binding or instability in the centrifugal pump provided the loop pressure was above 1.1 atm. The pump appeared to perform according to the characteristics shown in figure 18. These performance curves were determined as described in reference [2] and the load line of the entire flow loop was calculated from standard friction pressure drop equations. It should be noted that the load line does not change substantially for different densities in the pump. However, knowledge of the density in the pump is important in determining the mass flow rate.

In figure 19 the flow rate measured calorimetrically, \dot{m}_{exp} , is compared with that derived from the pump characteristics and the calculated load line, \dot{m}_{calc} . The density of the liquid was assumed to be that at the heat exchanger temperature and the measured loop pressure. The abscissa in figure 19 is the subcooling at inlet measured in watts. For subcritical pressures this is given by $\dot{m}_{exp}(H_{SAT} - H)$ where H_{SAT} is the enthalpy of saturated liquid at the loop pressure and H is the actual inlet enthalpy. For supercritical pressures H_{SAT} is taken to be the enthalpy corresponding to loop pressure and the transposed critical temperature. It is seen from the data available that the pump performed to within $\pm 15\%$ of its predicted performance at the higher pressures. The poor performance at 1.02 and 1.097 atm is attributed to vapor formation in the pump due to heat leak down the pump shaft. This is a special case of cavitation which is entirely dependent on the installation of the pump. We estimate a heat leak between 0.8 and 4.0 watts in the present installation which certainly explains the

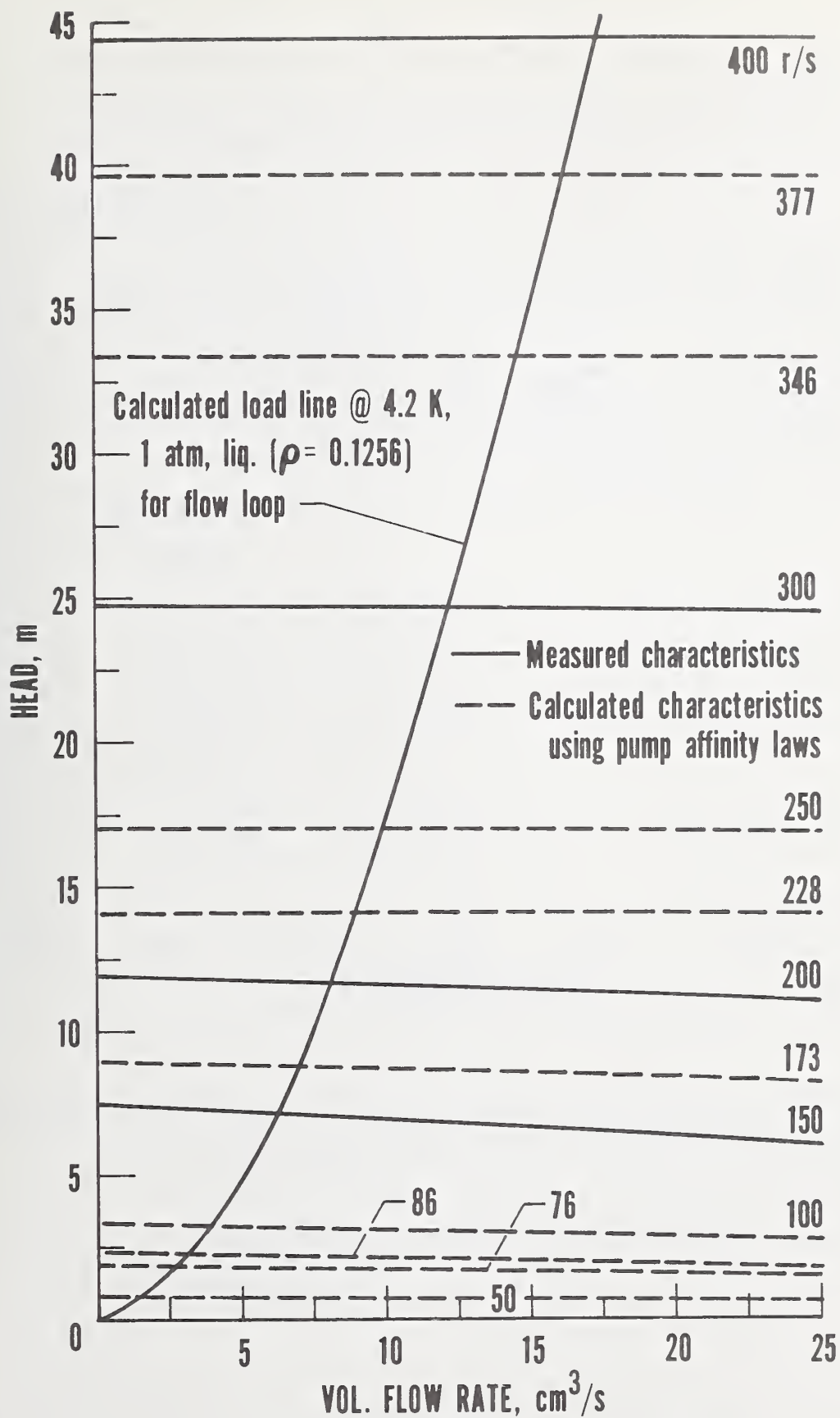


Figure 18. Pump performance characteristics and flow loop load line.

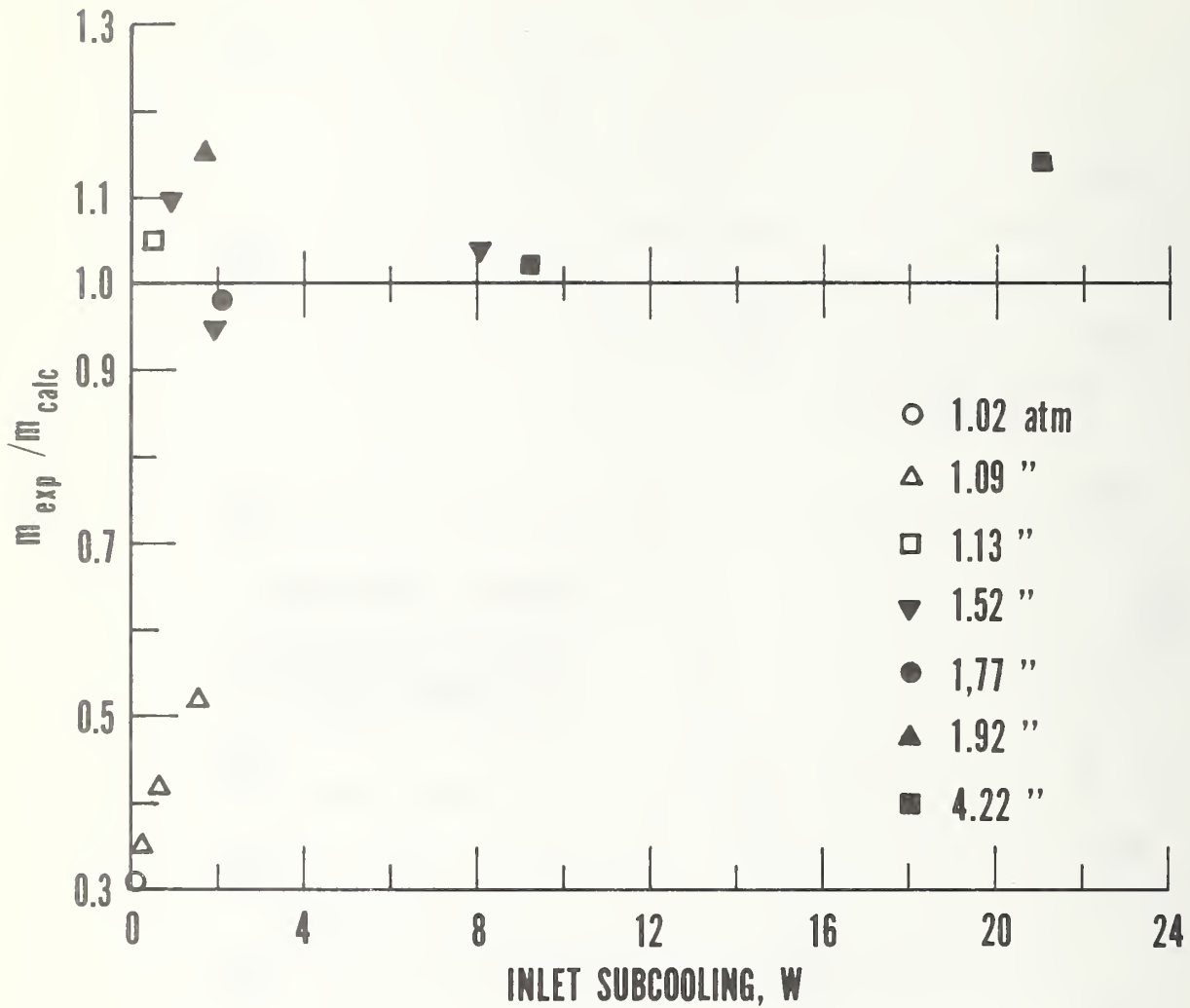


Figure 19. Ratio of measured flow rate to flow rate predicted from centrifugal pump performance characteristics vs subcooling power.

poor performance at 1.02 and 1.097 atm. However, at higher pressures the pump appeared to perform in spite of the heat leak and this is not entirely understood.

5. CONCLUSIONS

- i. The usual transition from wetted-wall to dry-wall heat transfer is observed in heat transfer to subcritical helium I under forced convection.
- ii. Below the transition, forced convection has little effect on heat transfer and the pool boiling correlation of Kutateladze for the heat flux vs. temperature rise of the wall is sufficient.
- iii. Above the transition, the heat transfer coefficient falls off drastically. For superconductivity applications this will usually have to be avoided except at mass velocities of the order of $60 \text{ g/cm}^2 \text{ s}$ or higher.
- iv. Transition is a function of many variables (see 3.2). More work will be required to make this a predictable phenomenon.
- v. At heat fluxes between 0.01 and 0.3 W/cm^2 , subcritical heat transfer is superior to supercritical for the same mass velocity. Above about 0.3 W/cm^2 the reverse is true.
- vi. The centrifugal pump used to circulate the liquid performed according to the characteristics determined earlier provided that below 1.1 atm the subcooling power was not less than about 2 W.

6. REFERENCES

- [1] Giarratano, P. J., Arp, V. D. and Smith, R. V., Forced convection heat transfer to supercritical helium, *Cryogenics*, 11, 385 (1971).
- [2] Sixsmith, H., and Giarratano, P. J., A miniature centrifugal pump, *Rev. Sci. Inst.* 41, 1570 (1967).
- [3] Johannes, C. and Mollard, J., Nucleate boiling of helium I in channels simulating the cooling channels of large superconducting magnets, *Adv. Cry. Eng.*, 17, 333 (Plenum Press 1972).
- [4] Keilin, V. E., Klimenko, E. D. and Kovalev, I. A., Apparatus for measuring hydraulic resistance and heat transfer in the two-phase flow of helium, RTS 5062, National Lending Library for Science and Technology, Boston SPA, Yorkshire (1968).
- [5] Jergel, M. and Stevenson, R., Heat transfer to liquid helium in narrow channels with laminar and turbulent flow, *Applied Phys. Letters*, 17, No. 3, (Aug 1970)
- [6] James, G. B., Lewis K. G., and Maddock, B. J., Critical heat fluxes for liquid helium boiling in small channels, *Cryogenics* 10, 481 (1970).
- [7] Kutateladze, S. S., Heat transfer in condensation and boiling, State Sci. and Tech. Pub. of Lit. on Machinery, Moscow (AEC translation 3770, Tech. Info. Service, Oak Ridge, Tenn.)
- [8] Brentari, E. G. and Smith, R. V., Nucleate and film pool boiling design correlations for O₂, N₂, H₂, and He., *Int. Adv. in Cry. Eng.*, 10 Part 2, 371 (Plenum Press, N. Y., 1965).

DOCUMENT CONTROL DATA - R & D

(Security classification of title, body of abstract and indexing annotation must be entered when the overall report is classified)

1. ORIGINATING ACTIVITY (Corporate author) Cryogenics Division National Bureau of Standards Boulder, Colorado 80302		2a. REPORT SECURITY CLASSIFICATION UNCLASSIFIED									
		2b. GROUP									
3. REPORT TITLE Forced Convection Heat Transfer to Subcritical Helium I											
4. DESCRIPTIVE NOTES (Type of report and inclusive dates) Final Report											
5. AUTHOR(S) (First name, middle initial, last name) Patricia J. Giarratano, R. C. Hess, and M. C. Jones											
6. REPORT DATE May 1973	7a. TOTAL NO. OF PAGES 36	7b. NO. OF REFS 8									
8a. CONTRACT OR GRANT NO. MIPR FY14557200411	9a. ORIGINATOR'S REPORT NUMBER(S) NBSIR 73-322										
b. PROJECT NO. c. 31453207 d.	9b. OTHER REPORT NO(S) (Any other numbers that may be assigned this report) AFAPL-TR-73-37										
10. DISTRIBUTION STATEMENT Approved for public release; distribution unlimited.											
11. SUPPLEMENTARY NOTES		12. SPONSORING MILITARY ACTIVITY Air Force Aero Propulsion Laboratory Wright-Patterson AFB, OH 45433									
13. ABSTRACT Preliminary results of an experimental investigation of heat transfer to liquid helium under forced flow conditions are reported for a 0.213 cm i. d. x 10 cm long test section subject to the following range of operating conditions: <table style="margin-left: 40px;"> <tr> <td>System pressures</td> <td>1.1 - 2.1 atm</td> </tr> <tr> <td>Mass velocities</td> <td>4 - 64 g/s-cm²</td> </tr> <tr> <td>Heat fluxes</td> <td>0.04 - 0.53 W/cm²</td> </tr> <tr> <td>Inlet subcooling</td> <td>0.03 - 0.10 K</td> </tr> </table> The effect of the above system parameters on the heat transfer and critical heat flux is discussed; a comparison of forced convection boiling with other modes of heat transfer (pool boiling and supercritical) and the performance of a centrifugal pump used for circulating the liquid helium are also included in the report.				System pressures	1.1 - 2.1 atm	Mass velocities	4 - 64 g/s-cm ²	Heat fluxes	0.04 - 0.53 W/cm ²	Inlet subcooling	0.03 - 0.10 K
System pressures	1.1 - 2.1 atm										
Mass velocities	4 - 64 g/s-cm ²										
Heat fluxes	0.04 - 0.53 W/cm ²										
Inlet subcooling	0.03 - 0.10 K										

14.

KEY WORDS

LINK A

LINK B

LINK C

ROLE

WT

ROLE

WT

ROLE

WT

Centrifugal pump
Critical heat flux
Film boiling
Forced convection
Heat transfer
Helium
Nucleate boiling
Subcritical
Supercritical



